

**Northwest Africa (NWA) 7034
(+7475, 7533, 7906, 7907, 8114, 8171, 8674)**

320 g (80.2, 84, 47.68, 29.94, 1.9, 81.88, 12 g)

Brecciated Shergottite

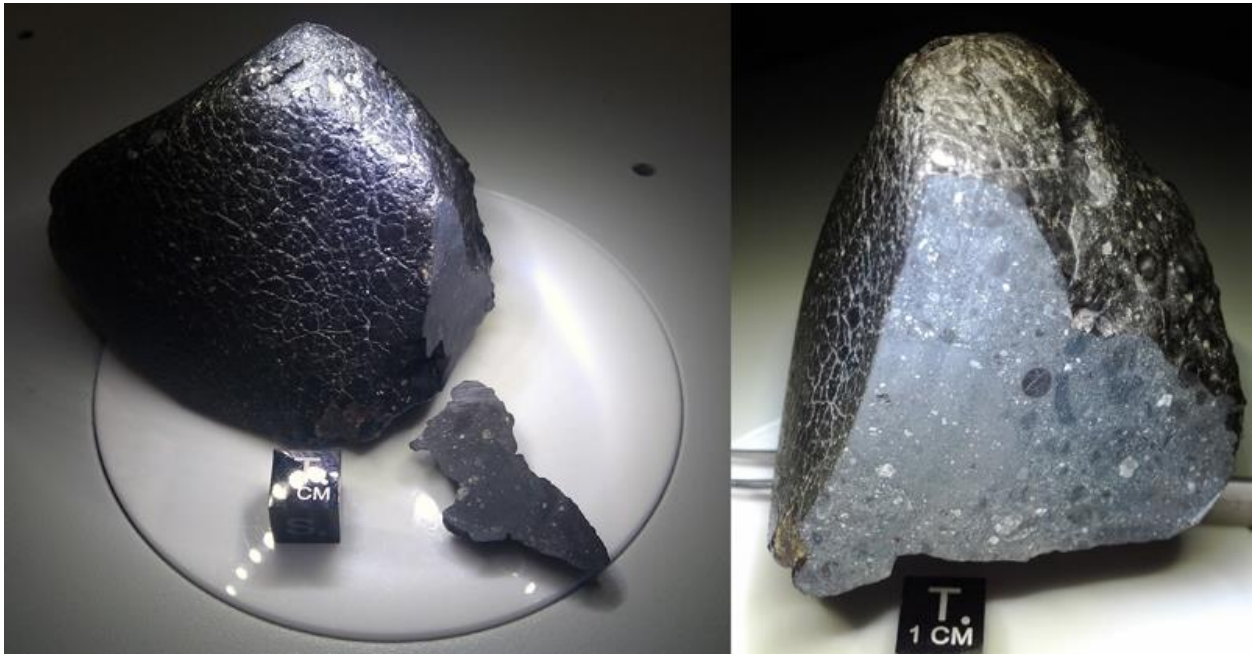


Figure 1 and 2: NWA 7034 showing fusion crusted exterior (left) and sawcut revealing interior (right), both images with a 1 cm cube for scale (courtesy of Institute of Meteoritics, UNM).

Introduction

Originally classified as an ungrouped achondrite, Northwest Africa 7034 was recovered and subsequently purchased in Morocco in 2011 (MB 100). From the original description “Single stone, shiny, black surface, saw cut reveals porphyritic breccia with numerous dark and light colored phenocrysts and clasts of variable size and texture, set in a dark groundmass, many reflective opaques visible.” It has a smooth surface (Figure 1) and a clastic interior (Figure 2). Subsequent analysis revealed NWA 7034 is of martian origin (MB101; Agee et al., 2012) and is actually a water-rich breccia (Agee *et al.* 2012). It has unusually high, fractionated oxygen isotope ratios. Since its finding 7 additional masses have been recognized, as described below.

NWA 7475 was purportedly recovered at the find site for NWA 7034 near Bir Anzarane, southern Morocco in 2012. Purchased by Luc Labenne from a Moroccan dealer in September 2012, it is a black, partly fusion-crust stone (80.2 g) consisting of black and white angular clasts plus dark spheroidal objects in a black matrix (MB102). NWA 7533 was purchased by LaBenne and type specimen resides at MNHP (MB101). NWA 7906

(47.68 g) and NWA 7907 (29.94 g) were purchased in January 2013 by Marc Jost in Morocco. Both are black stones with remnants of fusion crust, whereas the interior has light-colored clasts and spheroidal objects in a brecciated matrix (MB102). NWA 8114 is a fusion crusted stone, 1.8 cm length, and contains some terrestrial carbonate veining visible on the surface and in thin section. Some clasts also show through the fusion crust. NWA 8171 was purchased in June 2013 in Ensisheim, France (MB103). It is a nearly completely black 81.88 g stone with remnants of fusion crust, whereas the interior has light-colored clasts and spheroidal objects in a brecciated matrix. Finally, NWA 8674 was purchased by Jay Piatek from Morocco in 2012 (MB103). It is a single stone, with a shiny, black exterior. A saw cut reveals it is a breccia with numerous dark and light colored fragmental crystals and polycrystalline lithologies, scattered spherules and spherical objects of variable size and texture, set in a dark gray, fine-grained groundmass with some opaques visible.

Petrography

Agee et al. (2012) and MB 100 described NWA7034 as a “porphyritic basaltic breccia with phenocrysts of dominant andesine, low-Ca pyroxene, pigeonite and augite set in a very fine-grained, clastic to plumose, groundmass with abundant magnetite”. It also has “accessory sanidine, anorthoclase, apatite, chromite, ilmenite and pyrite”. Poikilitic pyroxene-plagioclase clasts and quench melt clasts present. No Fe-Ni metal observed. An updated petrography provided more detail and assigned the name porphyritic basaltic monomict breccia, and noted maghemite as well as magnetite in the groundmass. X-ray diffraction analyses revealed modal mineralogy of plagioclase feldspar ($38.0 \pm 1.2\%$), low-Ca pyroxene ($25.4 \pm 8.1\%$), clinopyroxenes ($18.2 \pm 4.0\%$), iron-oxides ($9.7 \pm 1.3\%$; 70% magnetite and 30% maghemite), alkali feldspars ($4.9 \pm 1.3\%$), apatite ($3.7 \pm 2.6\%$), and a minor amount of iron-sulfide and chromite. Detailed petrography of the other masses are presented below.

NWA 7475 was described in MB102 as a “complex breccia composed of angular to rounded mineral clasts, lithic fragments, and spheroidal objects (up to 5 mm in diameter), in a fine grained, dark matrix rich in magnetite.” Other minerals present include orthopyroxene, pigeonite, subcalcic augite, augite and hedenbergite, sodic to intermediate plagioclase, Ti-bearing magnetite, chlorapatite, ilmenite, pyrite, maghemite, hematite, alkali feldspar, anorthoclase, rutile, and monazite. Many clasts exhibit 50 μm -thick mantles of concentrically aligned, accreted debris $>5 \mu\text{m}$ in size. Clast types range from monomineralic feldspar and pyroxene fragments $<1 \text{ mm}$ size to polymineralic clasts that are aphanitic-glassy (some with igneous contacts to the host matrix). Crystallized melt clasts have textures ranging from sub-ophitic to ophitic, granular and poikilitic with grain sizes of plagioclase and pyroxene $<0.5 \text{ mm}$. Some spheroidal objects are composed of glass or fine grained quench assemblages, whereas others consist of concentrically zoned grain aggregates with radial shrinkage fractures (from MB102).



Figure 3: NWA 7034 ; photo credit, C. Agee, Institute of Meteoritics, UNM.



Figure 4: NWA 7475; photos from D. Weir (<http://meteoritestudies.com/>)



Figure 5: NWA 7533; top photo courtesy of Luc Labenne (Labenne Meteorites; <http://www.meteorites.tv/542-nwa-7533>), middle photo courtesy of Luc Labenne (from Ars Technica article; <https://arstechnica.com/science/2013/11/4-4-billion-year-old-meteorite-nwa-7533-is-straight-outta-mars/>), and bottom photo courtesy of Luc Labenne (from Nature article; http://www.nature.com/nature/journal/v503/n7477/fig_tab/nature12836_F1.html).



Figure 6: NWA 8171; top photo courtesy of Gregor H. http://www.encyclopedia-of-meteorites.com/test/58684_29740_2666.jpg; bottom photo courtesy of Luc Labenne (Labenne Meteorites; <http://www.meteorites.tv/542-nwa-7533> and http://www.encyclopedia-of-meteorites.com/test/58684_29563_2633.jpg).

NWA 7533 was described in MB101 as a breccia, with the largest objects (~1 cm) being flattened, oval or curved fine-grained melt bodies containing crystal fragments, often with melt mantles or coatings. The melt rocks in NWA 7533 also have a fine-grained subophitic to fasciculate texture (grain size 2-5 μm) with clots of central oxides (magnetite, chromite or ilmenite) in a mass of pyroxene dendrites embedded in aureoles of plagioclase. Crystalline clasts (up to ~2 mm) are dominated by pyroxenes and feldspars, with lesser magnetite and chlorapatite. There are also small coarse-grained noritic-monzonitic fragments, microbasalts, and melt spheres. Rare pyrite is replaced by magnetite and hydrated or oxidized magnetite.

NWA 7906, 7907, and 8171 are described as “breccias of angular mineral grains (up to 4 mm), lithic clasts and spheroidal objects (2-5 mm diameter) in fine-grained matrix.

Minerals observed are pyroxenes, plagioclase, alkali feldspar, magnetite, chlorapatite, ilmenite, pyrite, maghemite, and goethite (MB102; MB103).

NWA 8114 “has a clastic texture with augite and pigeonite ($\text{En}_{32-69}\text{Fs}_{19-44}\text{Wo}_{1.5-38}$), predominantly andesine plagioclase but also K-rich feldspar ($\text{An}_{15-60}\text{Ab}_{38-76}\text{Or}_{1.8-10}$ and $\text{Ab}_{22-41}\text{Or}_{59-78}$), Cl-apatite and Ti-magnetite.” (MB 102), similar compositionally to those reported in Agee et al. (2013) for NWA 7034. In addition, it contains zoned and rounded basaltic mineralogy and monomineralic (pyroxene, feldspar) clasts, similar to those reported in NWA 7034.

NWA 8674 is a polymict breccia with mostly fragmental but a few euhedral feldspar and pyroxene crystals up to 5 mm (MB103). Clast types include basaltic, trachytic, andesitic, and phosphate-rich, whereas spherules are iron-oxide-rich and silicate-rich. Together with some spherical matrix-rich objects, all of these are set in a very fine-grained groundmass of feldspar, pyroxene, oxides, phosphates, zircon, and sulfide. In addition, there are ubiquitous larger grains of magnetite + maghemite, Cl-apatite, chromite, and ilmenite throughout.

Clast types

Variety in clast types has been documented in NWA 7034 (Santos et al., 2015; Udry et al., 2014), NWA 7475 (Wittmann et al., 2015) and in NWA 7533 (Hewins et al., 2017). Rock types include gabbros, apatite-ilmenite-K feldspar clusters, quenched melts and vitrophyres, magnetite-rich reaction spherules, various basaltic lithologies (micro-, fine-, and medium-grained). There are also numerous mineral fragments.

Santos et al (2015) report the presence of at least four different igneous lithologies (basalt, basaltic andesite, trachyandesite, and an Fe, Ti, and P (FTP) rich lithology; Table 1 and Figures 7-9). Because these lithologies do not appear to be related by fractional crystallization or other igneous process, NWA 7034 is a polymict breccia with clasts from several different and unrelated igneous sources. Udry et al. (2014) report an unusual, large, sub-rounded clast in NWA 7034 exhibiting a vitrophyric texture, with skeletal pyroxene and olivine with mesostasis (Figure 10).

Wittmann et al. (2015) report the presence of 79 clasts in their study of thin section of NWA 7475. Most of the clasts are vitrophyre melt clasts, with others being crystallized melt, feldspar, pyroxene and sedimentary (see Table 2).

Hewins et al. (2017) report various clast types including clast laden melt Rock (CLMR), spherules, microbasalts, noritic and monzonitic clasts, as well as mineral fragments of orthopyroxene, augite, augite-pigeonite, plagioclase and feldspar (Figure 11,12).

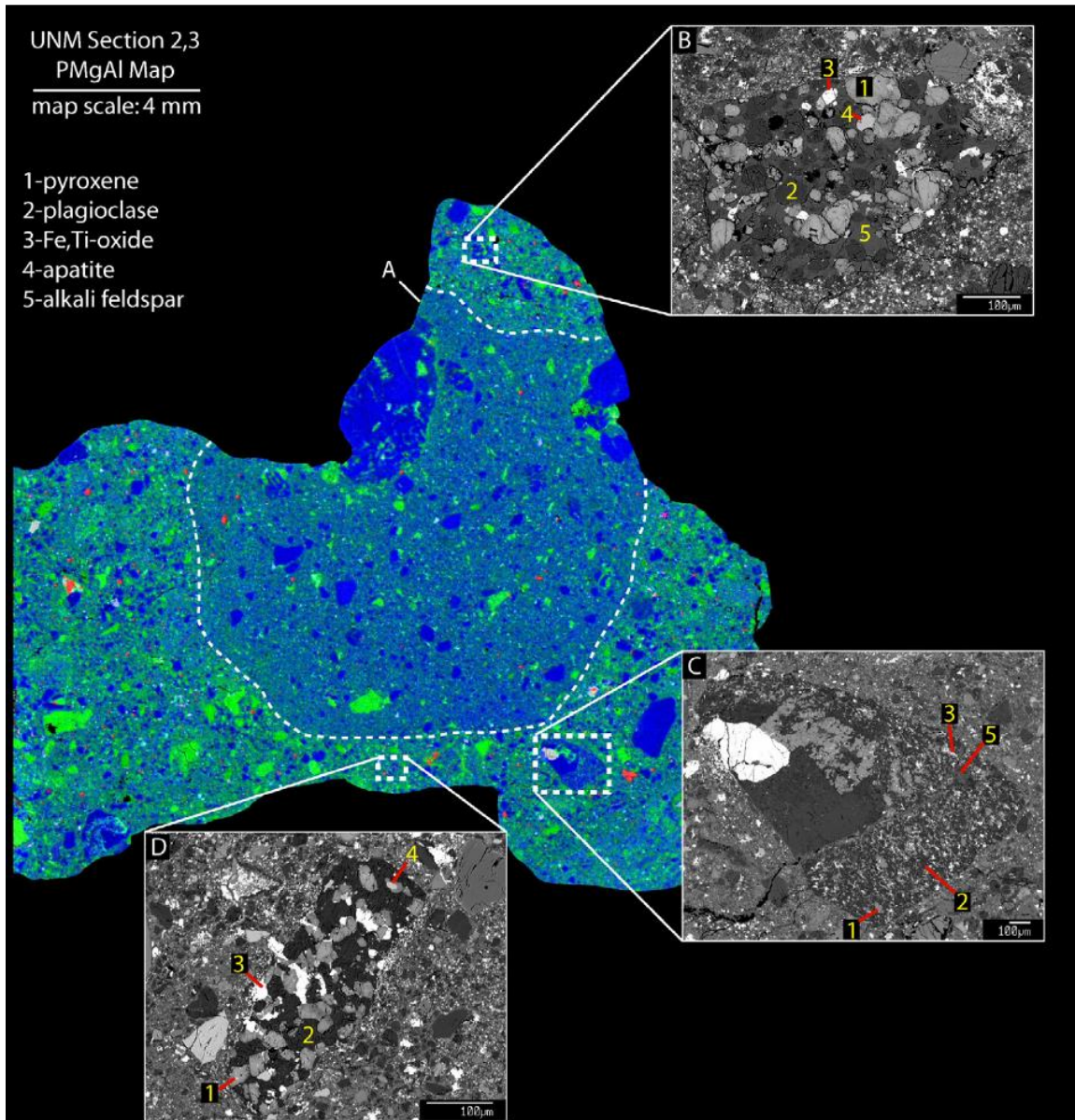


Figure 7: PMgAl X-ray map of UNM Section 2,3. P-red, Mg-green, Al-blue, Fe–Ti oxides and sulfides are white to gray. (A) Large protobreccia clast containing a distinct matrix from the bulk breccia, isolated mineral fragments of varying sizes, and igneous clasts. (B) Back scattered electron (BSE) image of Clast 76, a trachyandesite clast. (C) BSE image of Clast 74F, a trachyandesite clast. The coarse grained feldspar, pyroxene, and Fe–Ti oxide assemblage was not included in the study of this clast as it appears to represent a different lithology that is out of equilibrium with the surrounding fine grained clast material. (D) BSE image of Clast 73, a basalt clast (from Santos et al., 2015).

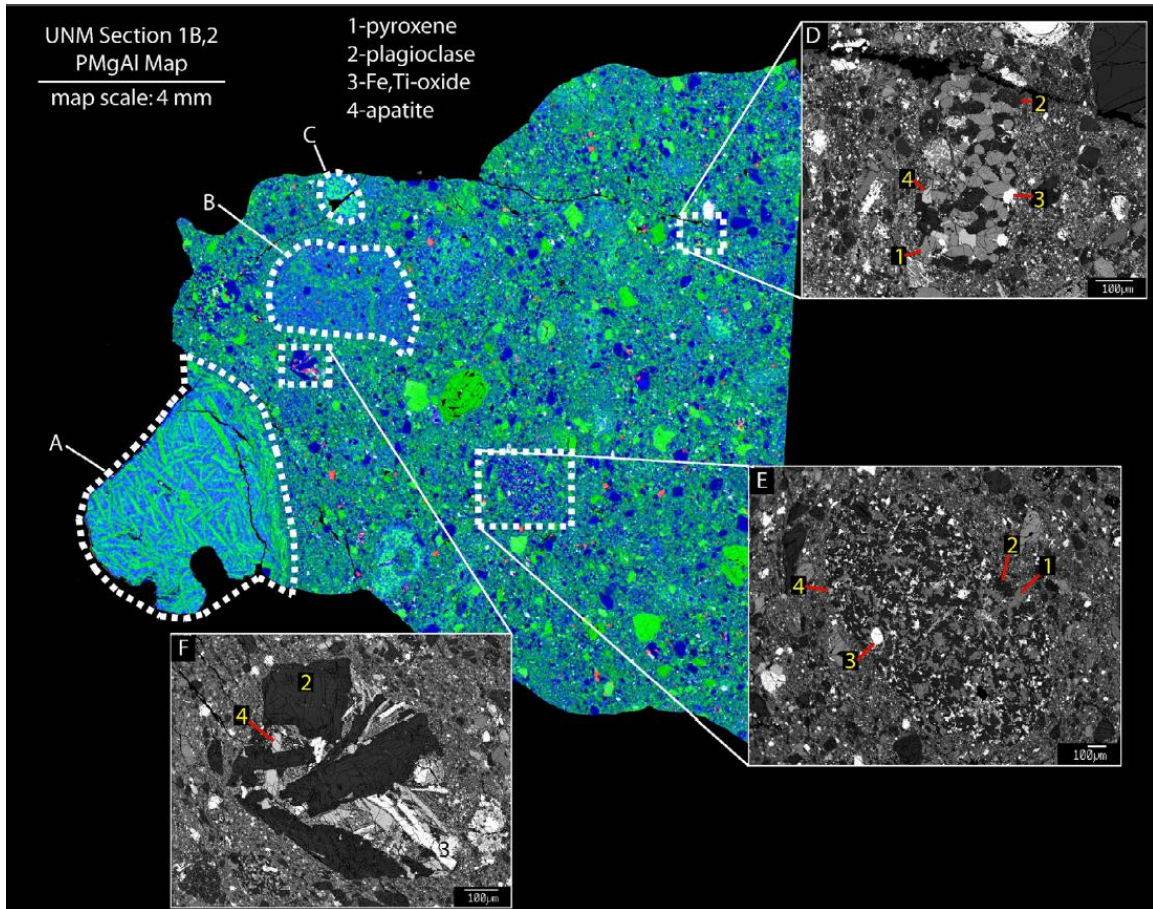


Figure 8: PMgAl X-ray map of UNM Section 1B,2. P-red, Mg-green, Al-blue, Fe–Ti oxides and sulfides are white to gray. (A) Impact melt clast, a portion of which was studied by Udry et al. (2014b). Note the skeletal but large mineral grains, indicating a rapid cooling but not quenching. The clast boundary in contact with the bulk matrix is rounded with aligned mineral grains roughly parallel to the boundary. BSE image highlighting the texture of this clast is in Fig. 8. (B) Proto-breccia clast, again having a matrix distinct from the bulk breccia matrix. (C) Altered, devitrified melt clast. (D) BSE image of Clast 5, a basalt clast. (E) BSE image of Clast 6, a basalt clast. (F) BSE image of FTP Clast 1, a phosphate and oxide rich clast. Note the extreme textural difference between the basalt and FTP clasts. (from Santos et al., 2015).

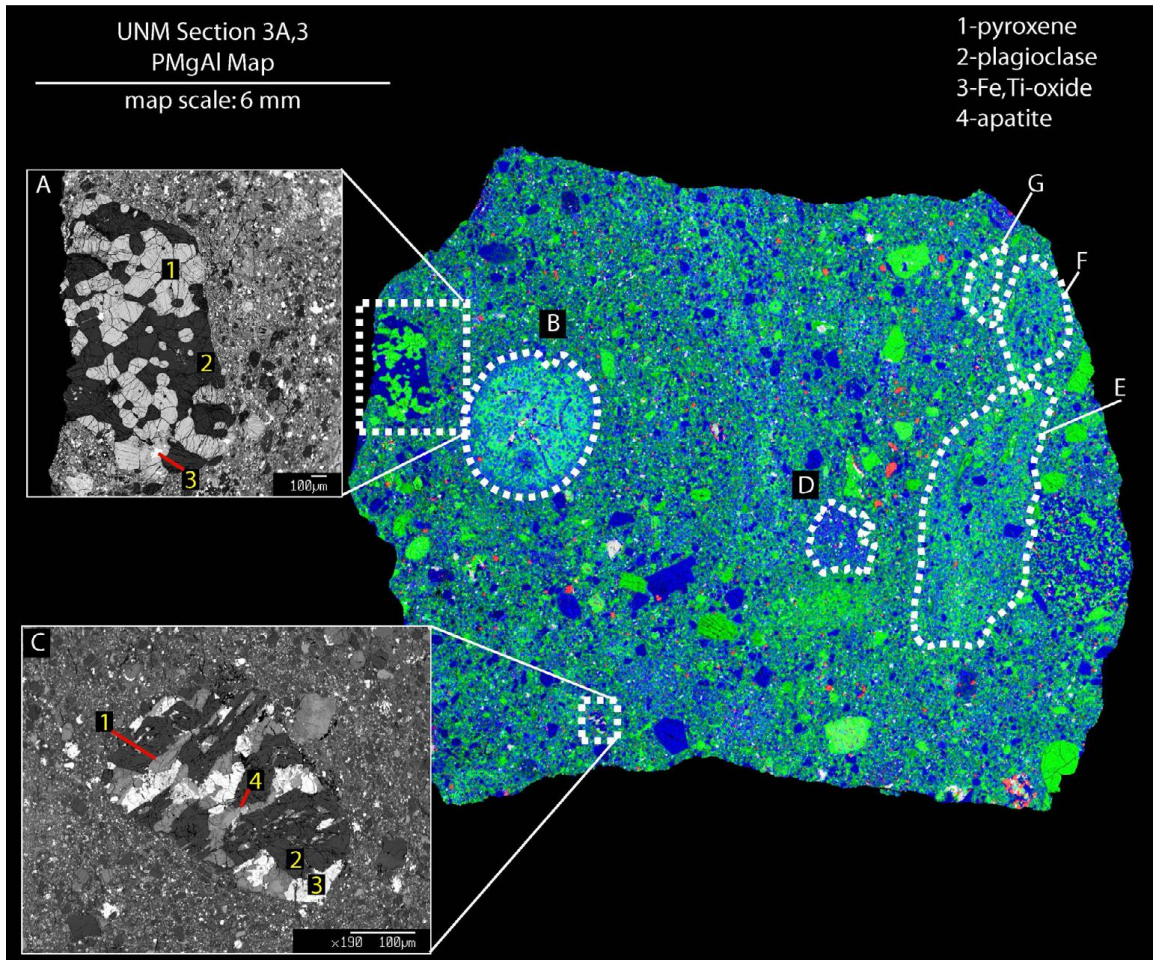


Figure 9: PMgAl X-ray map of UNM Section 3A,3. P-red, Mg-green, Al-blue, Fe-Ti oxides and sulfides shown in white to gray. (A) BSE image of Clast 1B, a parallel slice of Clast 1, a basaltic andesite clast. (B) An altered, devitrified melt clast. Close up BSE image of this clast is in Fig. 8. (C) BSE image of an FTP clast. This clast is one of few of this type to contain pyroxene. (D) Proto-breccia clast with a distinct matrix. (E-G) Lithic clasts containing matrix and larger mineral grains. These clasts do not appear very distinct from the bulk matrix, but they can be distinguished in BSE images. Further textural and chemical analysis is required to determine if these are altered melt clasts or proto-breccia clasts (from Santos et al., 2015).

Table 1: Clast types in NWA 7034 documented by Santos et al. (2015)

Summary of characteristics of different clast types observed in this study. Number of observations indicates number of clasts us distinguishing characteristics of the clast group.

Clast type (number of observations)	Distinguishing characteristics
Proto-breccia (4)	Fine grained matrix surrounding coarser grained mineral fragments and other types of clasts; distinct texturally or compositionally from bulk matrix. Matrix may contain different proportions and distributions of silicate phases, phosphates, and Fe-Ti oxides than bulk matrix
Melt clasts (7)	Contains devitrified glassy material or skeletal/plumose crystals, may contain relict grains. Devitrified mesostasis may contain numerous small Fe-Ti oxides, olivine may be present as skeletal/plumose crystals, common plagioclase and pyroxene crystals
Igneous clasts (30)	Interlocking mineral grains lacking matrix material. This clast group is subdivided into four separate groups listed below
Basalt clasts (19)	Basalt bulk composition. Textures include subophitic (with either strongly anhedral grains, subhedral grains, or irregular grains) and granulitic. Dominated by plagioclase and pyroxene with minor apatite and Fe-Ti oxides. Mg#s 53-62, $Fe^{3+}/\sum Fe$ 0.06-0.35
Trachyandesite clasts (3)	Trachyandesite bulk composition. Contain poikilitic texture and subophitic texture with irregular grain boundaries. Contain abundant K-feldspar typically poikilitically enclosing plagioclase. Mg#s 54-57, $Fe^{3+}/\sum Fe$ 0.08-0.29
Basaltic andesite clasts (2)	Basaltic andesite bulk composition. Granulitic texture. Very minor amounts of apatite and Fe-Ti oxides. Mg#s 57, 28, $Fe^{3+}/\sum Fe$ 0.03, 0.1
FTP clasts (6)	Basaltic texture. Relatively large apatite and Fe-Ti oxide grains tending towards euhedral morphologies; frequently lack pyroxene. P_2O_5 rich, Mg#~52 when containing pyroxene, ~10 when lacking pyroxene; $Fe^{3+}/\sum Fe$ ~0.24-0.38

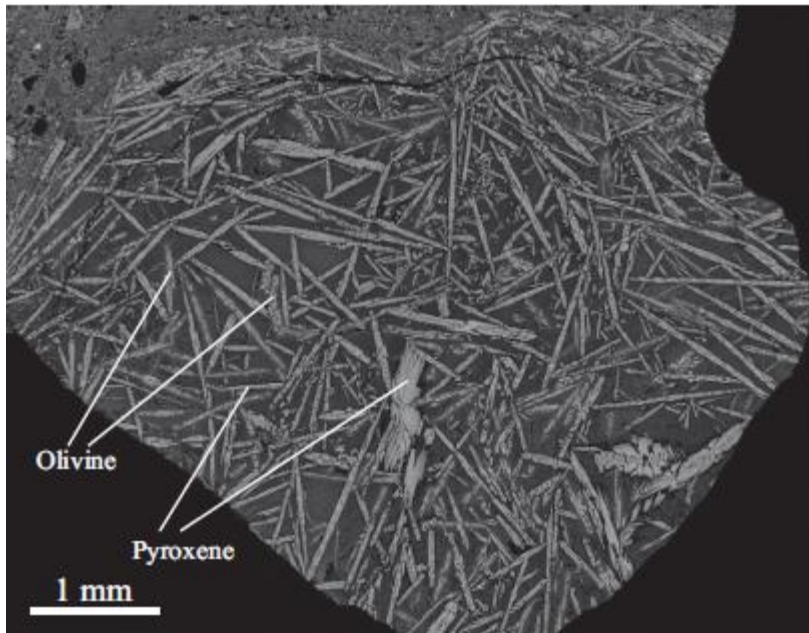


Figure 10: Udry et al. (2014) impact melt clast with vitrophyric texture.

Table 2: Clast types in NWA 7475 documented by Wittmann et al. (2015)

Clast type	N clasts	Area [mm ²]	Thin-section area [%] ^a	Clast area [%] ^b	Size range [mm ²]
Sedimentary	3	3.05	0.7	4.2	0.44-1.91
Pyroxene	10	1.96	0.5	2.7	0.12-0.43
Feldspar	4	0.78	0.2	1.1	0.11-0.33
Crystallized melt	22	12.80	3.0	17.5	0.11-2.59
Vitrophyre melt	40	54.44	12.6	74.5	0.11-5.58
Σ clasts	79	72.92	16.9	n.a.	0.1-5.6

^aProportion of the 432.65 mm² thin-section area.

^bProportion of the area sum of all clasts.

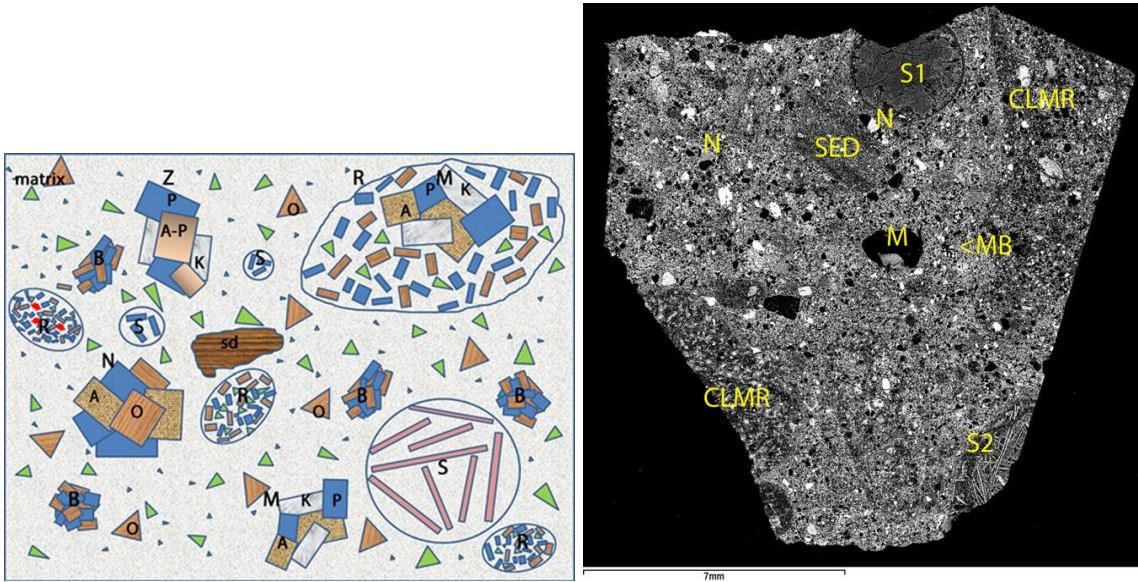


Figure 11 and 12: schematic sketch of components in NWA 7533 (left) and Mg Ka image of polished section NWA 7533-2, showing various clast types including a sedimentary lithology.

Mineralogy:

Mineral chemistry was reported in the initial descriptions from the Meteoritical Bulletin and summarized here in Table 3. In addition, minor phases were reported as follows:

Apatites

NWA 7034: apatite with $Cl=4.85\pm 0.34$ $F=0.70\pm 0.13$ $F+Cl=O$ 1.38 ± 0.06 (wt%) $n=16$,
 NWA 7533: apatite with 1.8 to 5.4 wt% Cl.

Sulfides

NWA 7475: pyrite (up to 2.8 wt.% Ni; $n=7$).

Olivine

NWA 8674: $Fa_{32.5\pm 0.7}$, $Fe/Mn=57\pm 4$, $NiO=0.009\pm 0.003$ (wt%), $n=2$.

Fragmental and igneous clast feldspars and pyroxenes in NWA 8674:

Large fragmental feldspars:

plagioclase $Ab_{51.4\pm 5.2}An_{46.4\pm 5.8}Or_{2.2\pm 0.6}$, $n=21$;
 K-feldspar $Ab_{13.4\pm 2.4}An_{2.0\pm 0.9}Or_{84.7\pm 3.1}$, $n=8$;
 albite $Ab_{88.4\pm 5.5}An_{4.3\pm 2.9}Or_{7.3\pm 3.1}$, $n=8$.

Igneous clast feldspars:

plagioclase $Ab_{60.5\pm 8.3}An_{36.4\pm 9.6}Or_{3.1\pm 1.5}$, $n=206$;
 K-feldspar $Ab_{20.0\pm 8.2}An_{3.0\pm 2.0}Or_{77.0\pm 9.6}$, $n=35$;

albite $\text{Ab}_{83.9 \pm 11.2} \text{An}_{7.3 \pm 6.0} \text{Or}_{8.8 \pm 6.1}$, n=23.

Large fragmental pyroxenes:

low-Ca pyroxene $\text{Fs}_{36.8 \pm 7.3} \text{Wo}_{3.7 \pm 0.4}$, Fe/Mn=33±3, n=19;

pigeonite $\text{Fs}_{40.3 \pm 5.9} \text{Wo}_{7.9 \pm 5.3}$, Fe/Mn=34±3, n=42;

augite $\text{Fs}_{34.9 \pm 9.3} \text{Wo}_{38.4 \pm 3.6}$, Fe/Mn=29±5, n=45.

Igneous clast pyroxenes:

low-Ca pyroxene $\text{Fs}_{35.2 \pm 5.7} \text{Wo}_{3.1 \pm 1.0}$, Fe/Mn=34±6, n=121;

pigeonite $\text{Fs}_{31.2 \pm 4.5} \text{Wo}_{10.1 \pm 3.9}$, Fe/Mn=34±4, n=81;

augite $\text{Fs}_{19.9 \pm 2.6} \text{Wo}_{40.9 \pm 5.1}$, Fe/Mn=33±6, n=32.

Table 3: Summary of mineralogy and mineral chemistry from Meteoritical Bulletin (MB) initial reports

Meteorite	MB#	orthopyroxene	pigeonite	clinopyroxene	plagioclase	oxide	Potassium feldspar
		FsWo, FeO/MnO	FsWo, FeO/MnO	FsWo, FeO/MnO			
NWA 7034	100,101	Fs _{31.6±6.7} Wo _{3.1±0.8} , 37±3	Fs _{35.5±3.5} Wo _{8.0±3.3} , 34±1	Fs _{24.3±4.5} Wo _{38.7±4.6} , 32±6	Ab _{52±6} An _{45±7} Or _{3±1}	I, M	Or ₇₇ Ab ₂₁ An ₃
NWA 7475	102	Fs ₁₉₋₄₈ Wo ₁₋₅ , 27-45	Fs ₂₅₋₄₄ Wo ₅₋₁₉ , 23-45	Fs ₁₇₋₃₀ Wo ₂₉₋₄₁ , 17-41 Fs ₉₋₁₈ Wo ₄₅₋₄₉ , 18-61 Fs ₃₇₋₄₄ Wo ₄₃₋₄₈ , 40-65	An ₁₀₋₅₈ Or _{1.9-6.8}	I, M	An _{0.8-13} Or ₅₃₋₉₀ Cn ₁₋₆ <i>Anorthoclase:</i> An ₂₂₋₂₆ Or ₁₀₋₂₀
NWA 7533	101	Fs _{21.9} Wo _{1.9} to Fs _{49.4} Wo _{5.0} , 34.6	Inverted pigeonite from Fs ₄₀ Wo ₂ with Fs ₂₁ Wo ₄₄ lamellae to Fs ₄₈ Wo ₆ with Fs ₂₁ Wo ₄₄ lamellae	Fs _{15.4} Wo _{40.5} to Fs _{30.5} Wo _{39.5}	An _{41±8} Ab _{56±7} Or _{3±1}	I, M, C, Mh	<i>Perthite:</i> An _{3±2} Ab _{22±7} Or _{74±9} and An _{4±2} Ab _{89±3} Or _{7±2} <i>Anorthoclase:</i> An _{5±2} Ab _{83±13} Or _{12±11} <i>Orthoclase:</i> An _{2±0} Ab _{21±1} Or _{77±1}
NWA 7906	102	Fs ₂₂₋₄₃ Wo ₂₋₄ , 25-40	Fs ₃₀₋₅₀ Wo ₆₋₁₃ , 30-42	Fs ₃₁₋₅₁ Wo ₃₈₋₄₈ , 22-42	An ₂₇₋₅₁ Or _{1.7-4.4}		An _{1.1} Or ₈₇
NWA 7907	102	Fs ₂₁₋₅₅ Wo ₂₋₅ , 26-55	Fs ₃₃₋₄₇ Wo ₇₋₁₈ , 34-52	Fs ₁₆₋₂₆ Wo ₃₇₋₄₅ , 28-36	An ₂₉₋₅₂ Or _{1.6-4.5}		An _{4.8} Or ₅₃
NWA 8114	102		En ₃₂₋₆₉ Fs ₁₉₋₄₄ Wo _{1.5-38}		An ₁₅₋₆₀ Ab ₃₈₋₇₆ Or _{1.8-10}		Ab ₂₂₋₄₁ Or ₅₉₋₇₈
NWA 8171	103	Fs _{21.3-45.6} Wo _{1.9-4.0} , 27-43	Fs _{30.9-37.1} Wo ₆₋₉ , 34-42	Fs _{8.4-29.7} , Wo ₃₈₋₄₅ , 13-41	An _{1.7-52.7} Or _{1.5-10.5}		An _{4.0} Or _{73.9}
NWA 8674	103						

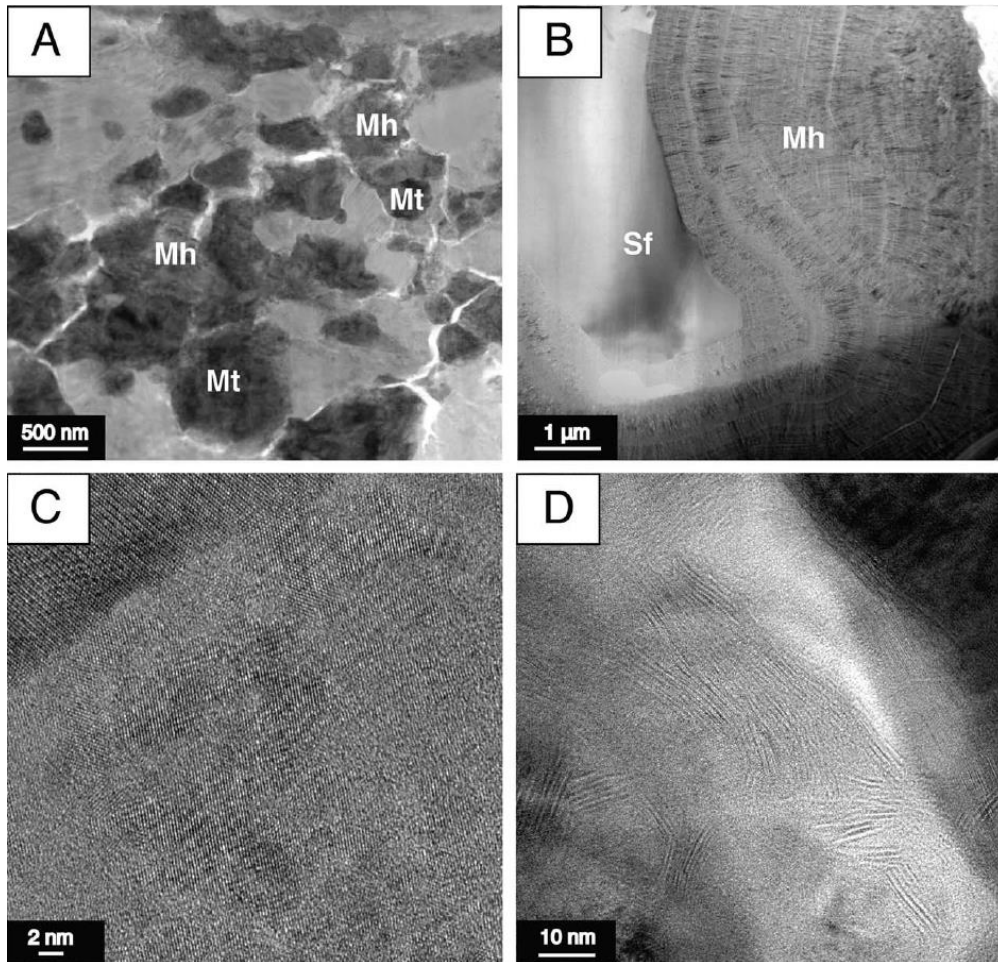


Figure 13: Muttik et al. (2014) maghemite (A to C) and saponite (D) were identified as primary OH-bearing phases in NWA 7034; these can account for 6000 ppm H₂O measured in bulk rock analysis.

Oxygen fugacity

Several aspects of the mineralogy of NWA 7034 and pairs indicate a very high oxygen fugacity. Ilmenite-magnetite pairs record temperatures and oxygen fugacities from 587 to 850 C, and FMQ to FMQ+4 (Agee et al. 2013; Santos et al. 2015).

Geochemistry

General / preliminary bulk composition

Initial bulk analyses of NWA 7034 and pairs revealed its Ni and Cr-rich nature (Ni = 494-550 ppm; Cr – 1485-1660 ppm, for NWA 7906, 7907, and 8171; MB102, 103). Overall Mg, Ni, and Fe/Mn are consistent with martian origin, although the elevated Ni contents are in indication of chondritic contamination from an impactor (see below; Figure 14). Whole rock analyses also exhibit light REE enrichment (Figure 15).

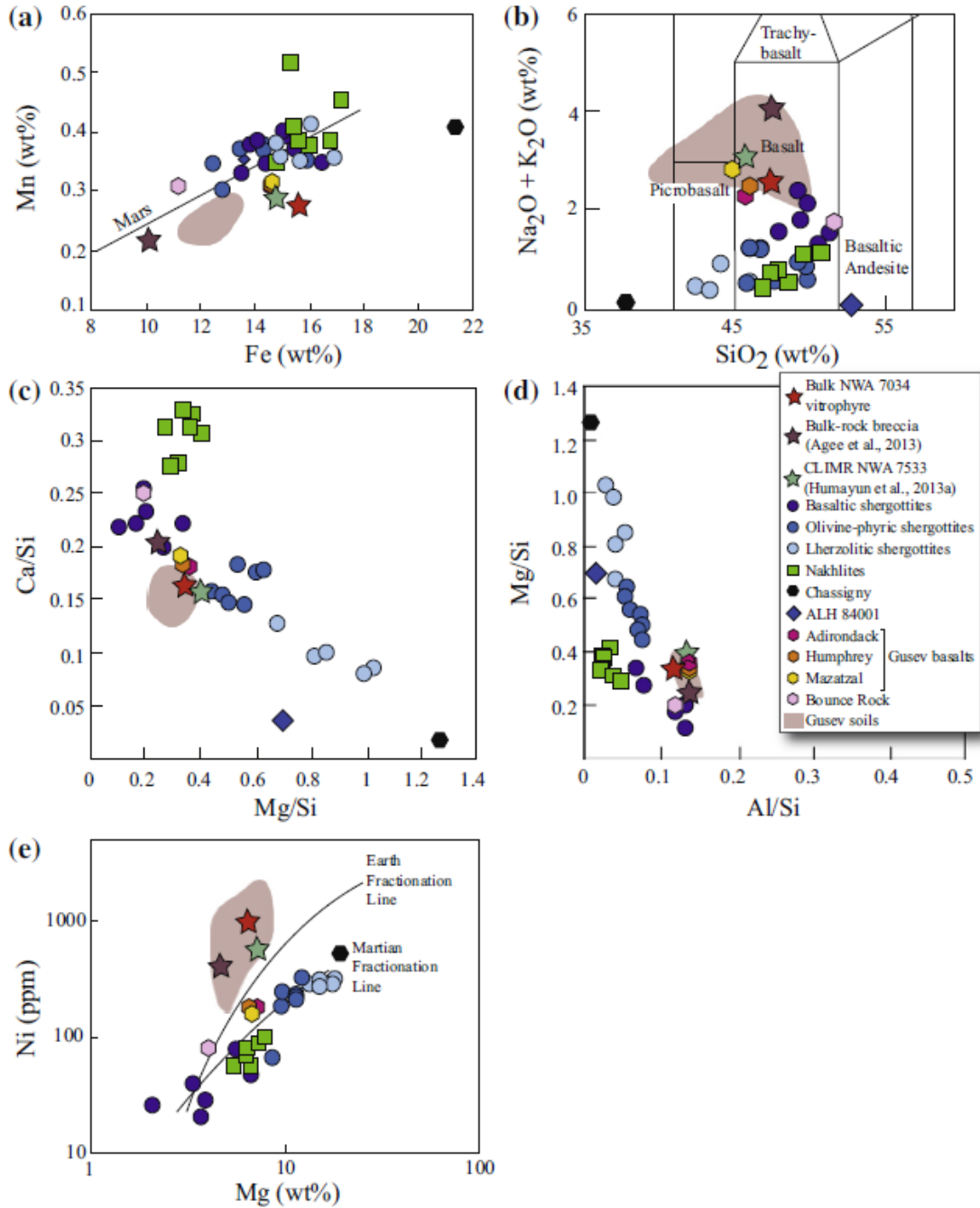


Figure 14: Udry et al. (2014) and Agee et al. (2013) bulk and clast compositions from NWA 7034, compared to other known martian lithologies.

Martian Breccia - NWA 7034

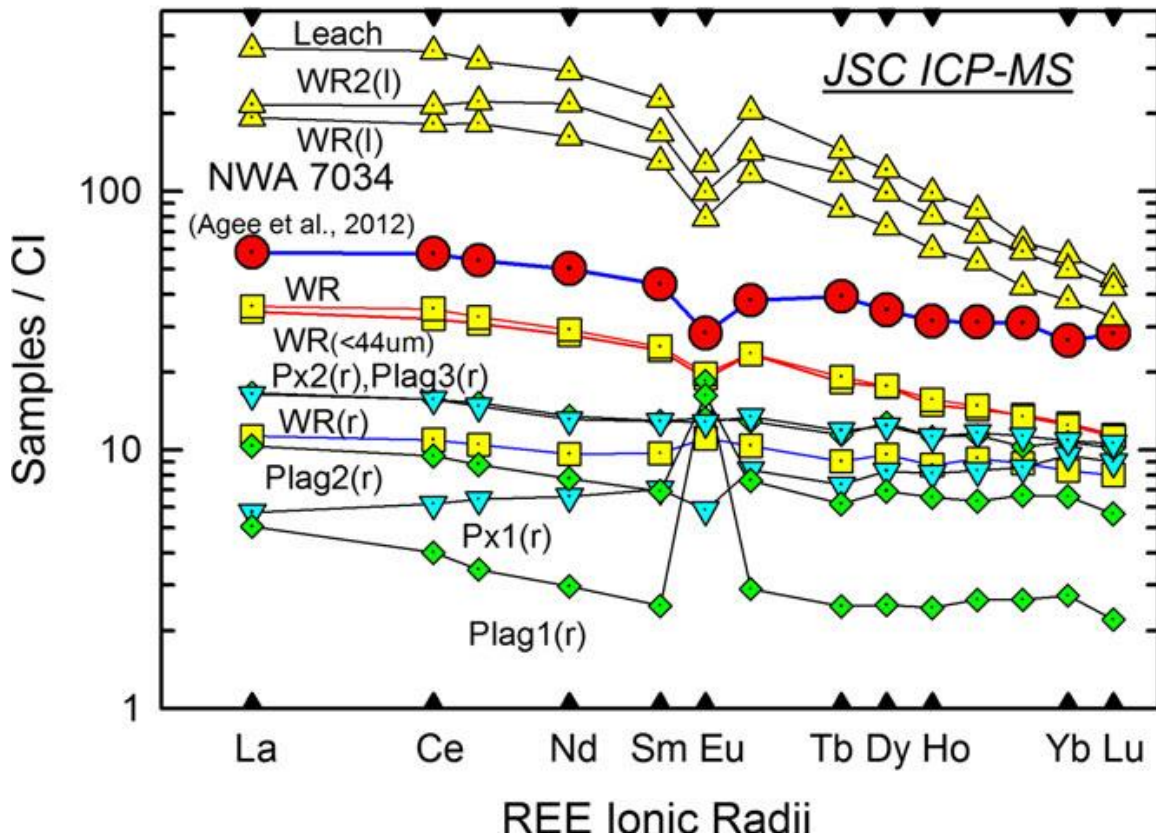


Figure 15: Bulk and mineral separate REE patterns measured by Nyquist et al. 2016 for NWA 7034.

Udry et al. (2014) report a very high Ni content (1020 ppm) in the vitrophyre melt clast from their study (Figure 14) – it is the highest measured in any known martian meteorite or martian igneous rock, suggesting an impact melt origin for the vitrophyre. Addition of 5.3–7.7% chondritic material to the target rock would account for the Ni enrichment. The bulk major and trace element abundances of the vitrophyre indicate that the protolith was not the host breccia nor any other martian meteorites. However, the clast is compositionally similar to Humphrey rock in Gusev crater analyzed by the Spirit rover and to a texturally distinct group of clasts in the paired meteorite NWA 7533. Udry et al. (2014) therefore propose that the target rock was an igneous lithology similar to Gusev basalts, which was subsequently contaminated by a chondritic impactor.

Santos et al. (2015) show that NWA 7034 basalt clasts and average bulk matrix most closely match compositions from Gusev Crater and the average martian crust determined by GRS. Basaltic andesite clasts fall in similar ranges as the TES field, while the trachyandesite and FTP clasts have no previously seen analogues (Figure 16). Some of the rocks seen in Gale Crater are even more alkali rich than clasts from NWA 7034. The SNC meteorites are not a match for any of the clast groups in this compositional space. The basalt lithologies are a good match for measured rock compositions from the martian

surface, however more exotic lithologies (e.g., trachyandesite and FTP lithologies) show this meteorite contains previously unsampled rock types from Mars. These new rock types provide evidence for a much greater variety of igneous rocks within the martian crust than previously revealed by martian meteorites, and supports recent rover observations of lithologic diversity across the martian surface. Furthermore, the ancient ages for the lithologic components in NWA 7034 indicate Mars developed this lithologic diversity in the early stages of crust formation (Santos et al., 2015).

The clast types in NWA 7533 (Hewins et al., 2017) are similar in composition to the clasts documented in other paired masses of NWA 7034. The three lithologies studied in detail by Hewins et al. (2017) – the microbasalt, monzonite, and melt rock, all show some affinity to the alkaline compositions seen in the other studies (such as trachybasalts and trachyandesites; Santo et al., 2015; Udry et al., 2014).

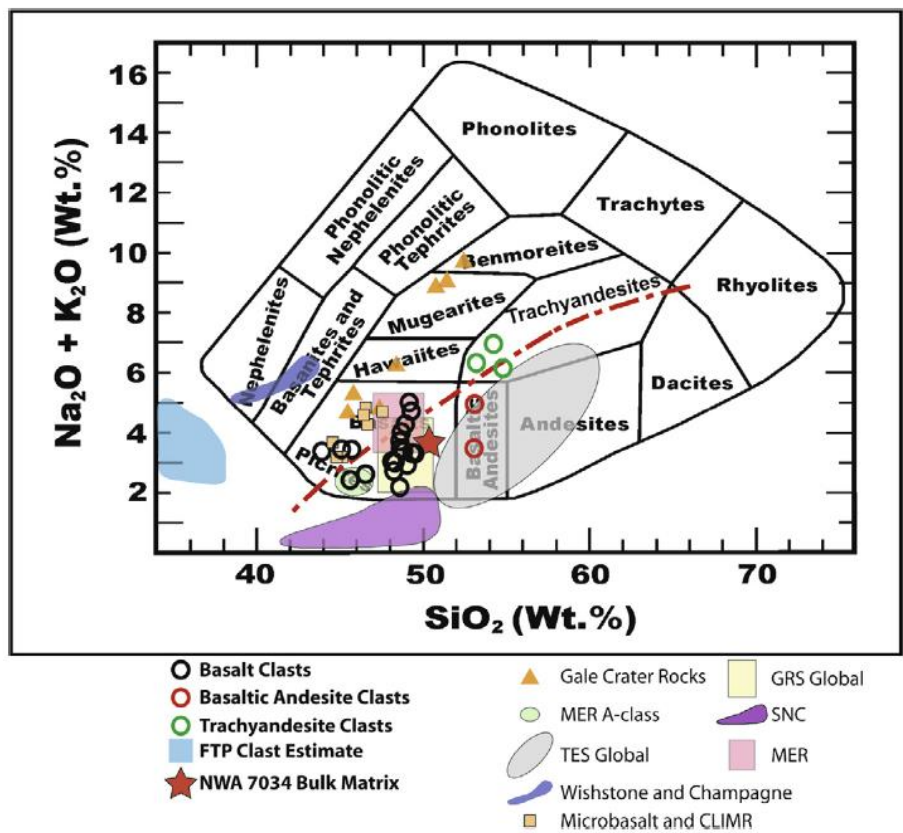


Figure 16: Bulk composition of NWA 7034 matrix and clast reported by Santos et al. (2015).

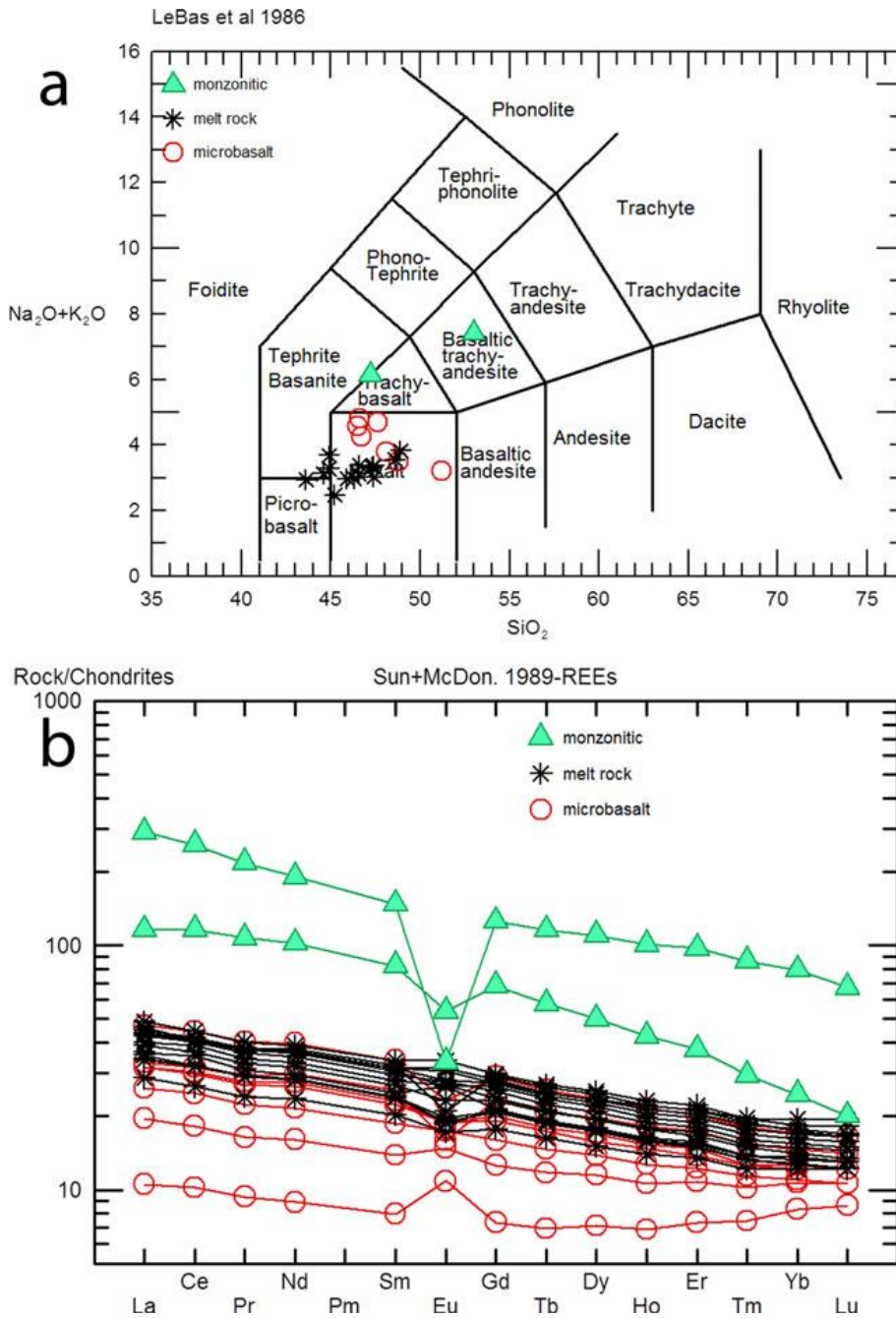


Figure 17: Clasts compositions found in NWA 7533 by Hewins et al. (2017).

Bulk rock chemical data for NWA 7475 (Wittmann et al., 2015) compared to the surface composition of Mars as measured by the Mars Odyssey gamma-ray spectrometer indicates a matching region in the southern highlands Terra Sirenum region centered at 30°S/165°W. This location agrees with petrologic and chronologic constraints for NWA 7475 and paired stones. A possible source crater for NWA 7475 and paired stones is ~5 Ma old, rayed Gratteri crater at 17.7°S, 160.1°W with an apparent diameter of 6.9 km.

Oxygen isotopes

Table 4: summary of oxygen isotopes on NWA 7034 and pairs

Sample	$\delta^{17}\text{O}$	$\delta^{18}\text{O}$	$\Delta^{17}\text{O}$	MB
NWA 7034	3.76, 3.52, 4.09, 3.89	6.00, 5.79, 6.51, 6.32	+0.59, +0.46, +0.65, +0.55	100,101
NWA 7475				102
NWA 7533	3.65	5.92	+0.57	101
NWA 7906	3.92	6.28	+0.62	102
NWA 7907	3.89	6.27	+0.60	102
NWA 8114	4.36	7.25	+0.59	102
NWA 8171	4.41(16)	7.18(31)	+0.675(1)	103

Oxygen isotopes are summarized in Table 4. 21 analyses of bulk NWA 7034 have been carried out. The mean value obtained at *UNM* was $\Delta^{17}\text{O}=0.58\pm 0.05\text{‰}$ $n=13$ for acid washed samples and $\Delta^{17}\text{O}=0.60\pm 0.02\text{‰}$ $n=6$ for non-acid-washed samples; at *UCSD* the mean value was $\Delta^{17}\text{O}=0.50\pm 0.03\text{‰}$ $n=2$ for vacuum pre-heated samples that were dehydrated and decarbonated. The combined data give $\Delta^{17}\text{O}=0.58\pm 0.05\text{‰}$ $n=21$. (Z. Sharp, K. Ziegler, *UNM*; M. Nunn, *UCSD*; MB101).

Oxygen isotopic values are shifted above the Mars fractionation line, even after consideration of hot desert weathering effects. Some values are consistent with other martian meteorites and may indicate a more standard origin from the martian interior. However, some values are nonetheless higher than the MFL and this has been interpreted as due to photolytic interaction with the martian atmosphere (Ziegler et al., 2013).

Prolonged interaction of martian lithosphere, hydrosphere and atmosphere is recorded in zircons from clasts in NWA 7034 (Figures 18 and 19). The variation measured in these four clasts can be explained if the mantle melts from which the zircon crystallized approximately 4.43Gyr ago had assimilated ^{17}O -enriched regolith materials, and that some of the zircon grains, while in a metamict state, were later altered by low-temperature fluids near the surface less than 1.7Gyr ago (Nemchin et al., 2014).

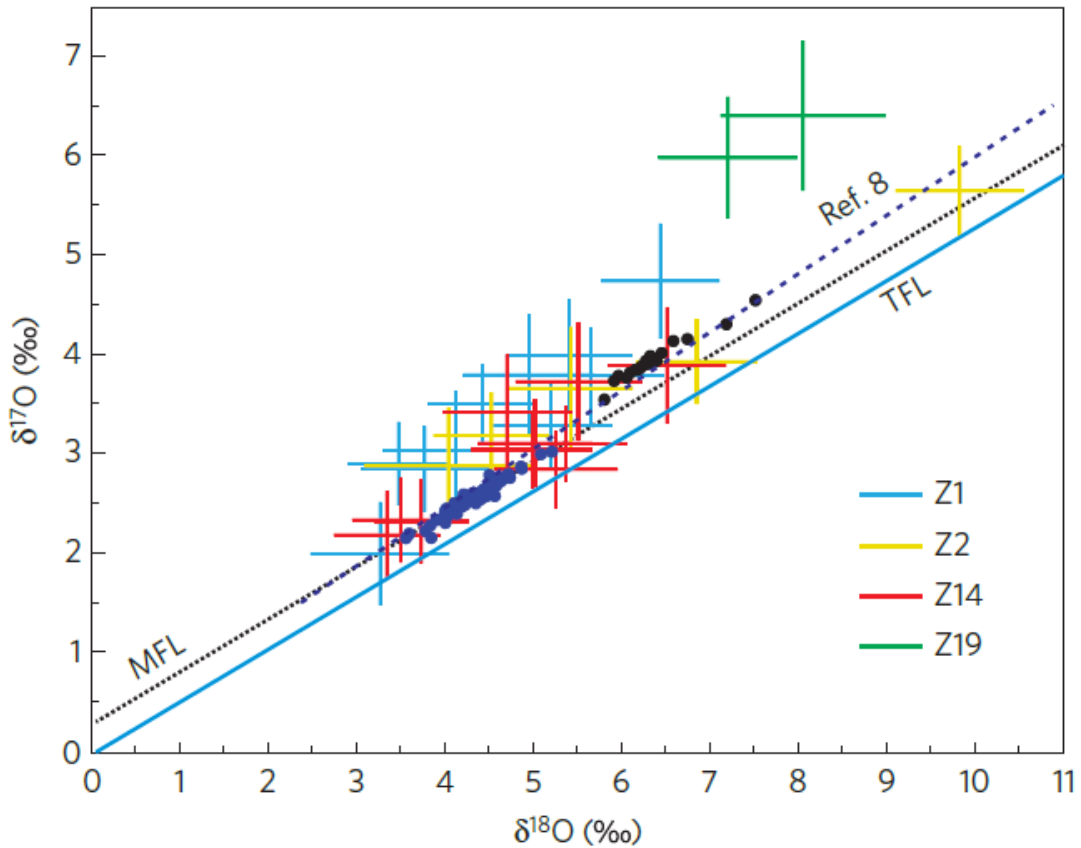


Figure 18: $\delta^{17}\text{O}$ versus $\delta^{18}\text{O}$ diagram showing results obtained for zircon grains from NWA 7533. Also shown are the terrestrial fractionation line (TFL; blue line), the martian fractionation line (MFL; black dotted line), the mixing line constrained from the analyses of rock-forming minerals from NWA 7034 (black dashed line; Zeigler et al., 2013), paired with the NWA 7533 (black circles; from Agee et al., 2013) and whole rock samples of SNC meteorites (navy circles; Farquhar et al., 1988; Franchi et al., 1999; Rumble and Irving, 2009).

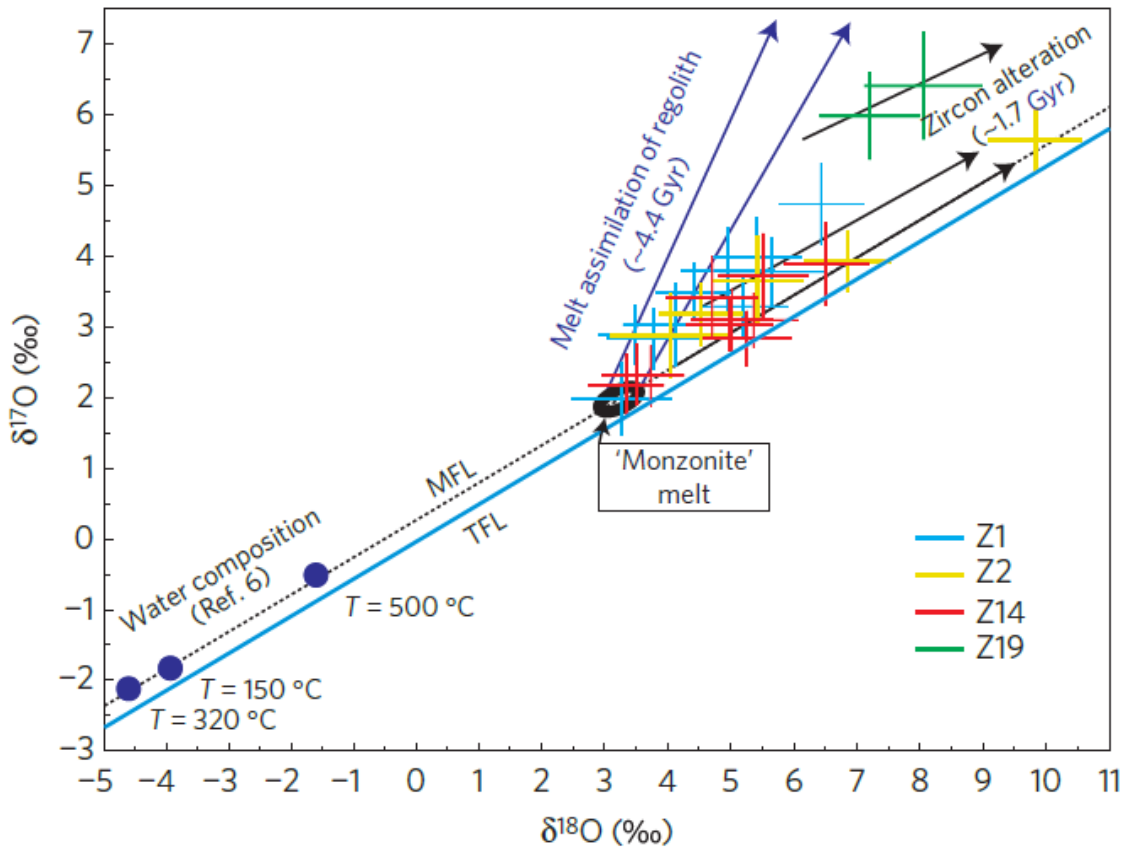


Figure 19: Nemchin et al. (2014): Black ellipse indicates zircon that would crystallize from the melt unaffected by assimilation and/or alteration; navy arrows indicate $\delta^{17}\text{O}$ formed as a result of the mixing of this melt with the surface materials enriched in ^{17}O (schematic, no specific endmember composition implied); black arrows indicate $\delta^{18}\text{O}$ correlated with the degree of radiation damage in different sub-domains of the grains formed as a result of exchange with the low-temperature hydrous fluids (converging to a single point where zircon would be completely equilibrated with the water).

Hydrogen isotopes

Hydrogen isotopes (Z. Sharp, K. Ziegler, UNM): six whole-rock combustion measurements yielded a bulk water content of 6190 ± 620 ppm. The mean δD value for the bulk combustion analyses was $+46.3 \pm 8.6$ ‰. The maximum δD values in two separate stepwise heating experiments were $+319$ ‰ and $+327$ ‰, reached at 804°C and 1014°C respectively.

Radiometric ages

Initial dating studies reported ages of ~ 2.1 Ga (Agee et al., 2013; MB100), generating excitement in the Mars science community since this is an age that is not common in the martian meteorite samples. However, follow up studies of a variety of

techniques have instead uncovered ages as old as 4.48 Ga and extending to much younger ages of 1.3 due to various processes of metamorphism, impact, and hydrothermal alteration (Yin et al., 2014; Tartese et al., 2014; Nemchin et al., 2013; Humayun et al., 2013; Bellucci et al., 2015; Nyquist et al., 2016; Agee et al., 2013).

Initially reported Rb-Sr data for NWA 7034 yielded an age of 2.089 ± 0.081 Ga (2σ). These whole rock Rb-Sr ages were initially interpreted as ~ 2.1 Ga age, but additional studies revealed a more complicated history of Rb-Sr in these meteorites (Nyquist et al., 2016). Sm-Nd on similar samples and subsplits have revealed ages that are ancient as well – 4.42 to 4.48 Ga (Nyquist et al., 2013; 2016) (Figures 20 and 21).

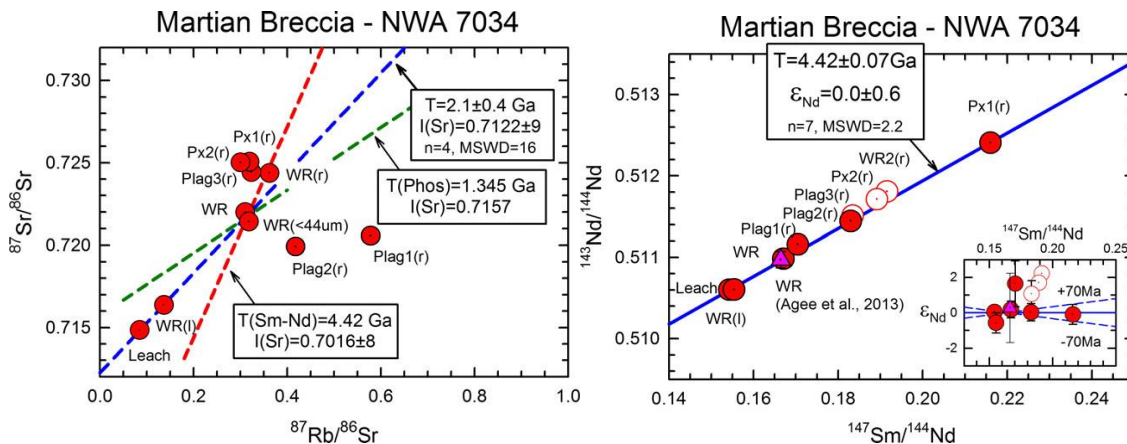


Figure 20: The Rb-Sr isotopic data do not define rigorous isochrons and indicate substantial disturbance (from Nyquist et al. 2016)

Figure 21: Sm-Nd analyses have been completed for three samples: bulk rock (WR), bulk rock leachate (WR(l)), and the residue after leaching of a pyroxene separate (Px1(r)). REE pat-terns determined by ICP-MS on 1% aliquots of the sample solutions (WR(l): La $\sim 200X$, LREE enriched; Px1(r): La $\sim 6X$, LREE depleted) verify the primary contributions to WR(l) and Px1(r) as phosphates and pyroxene, respectively. The REE pattern for WR is similar to that reported for the bulk rock by Agee et al. (2013), and the Sm-Nd data for WR agree with those reported by Agee et al. (2013) for a bulk sample. The isochron age for WR(l)+2WRs+Px1 gives an apparent age of 4.39 ± 0.08 Ga (MSWD=0.017). This isochron primarily dates pyroxene in NWA 7034, since the data for WR(l) and WR plot close together (from Nyquist et al. 2013, 2016).

Focused SIMS and MC-ICP-MS studies of zircons, feldspars, and baddeleyite have also yielded old ages from ~ 4.4 Ga to 1.3 Ga (Figures 22-24; Yin et al., 2014; Tartese et al., 2014; Nemchin et al., 2013; Humayun et al., 2013; Bellucci et al., 2015).

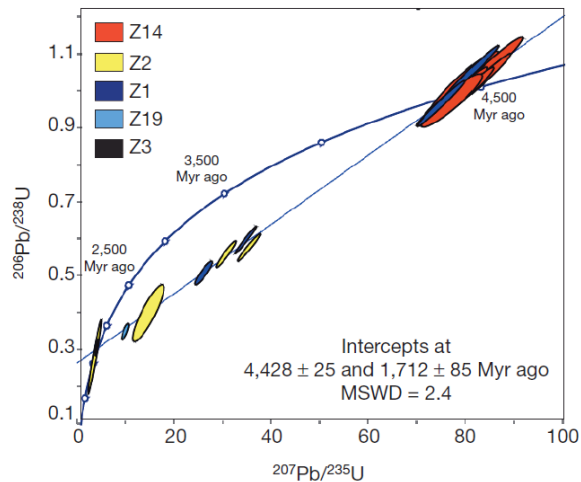


Figure 22: U-Pb ages from zircons in clasts from NWA 7034 (from Humayun, 2013).

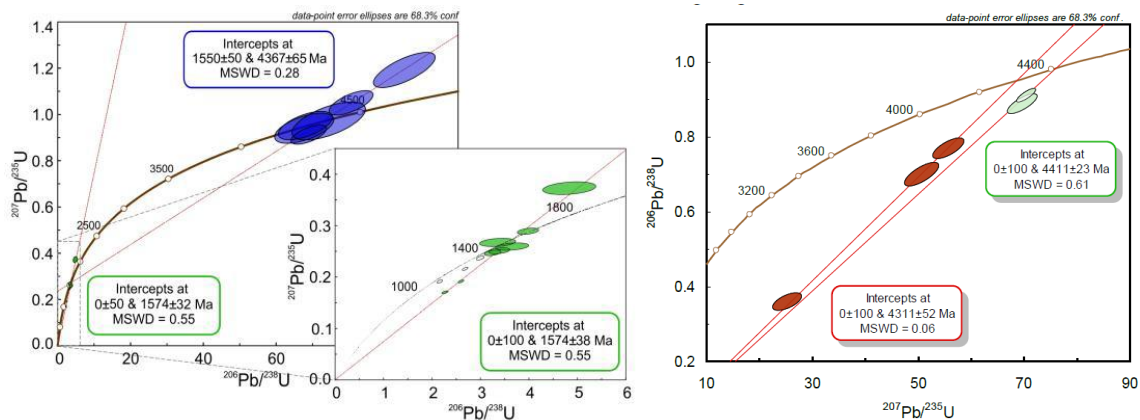


Figure 23: Tartese 2014 zircon (left)

Figure 24: Tartese 2014 baddeleyite (right)

Bellucci et al. (2015) measured the Pb isotopic compositions of NWA 7533 plagioclase and alkali feldspars, as well as U–Pb isotopic compositions of chlorapatite in the monzonitic clasts of NWA 7533 (Figure 25) by Secondary Ion Mass Spectrometry (SIMS). The U–Pb isotopic compositions measured from the chlorapatite in NWA 7533 yield an age of 1.357 ± 81 Ga (2σ). The least radiogenic Pb isotopic compositions measured in plagioclase and K-feldspar lie within error of the 4.428 Ga Geochron (Figure 26). These data indicate that the monzonitic clasts in NWA 7533 are a product of a differentiation history that includes residence in a reservoir that formed prior to 4.428 Ga with a μ -value ($^{238}\text{U}/^{204}\text{Pb}$) of at least 13.4 ± 1.7 (2σ) and a κ -value ($^{232}\text{Th}/^{238}\text{U}$) of ~ 4.3 . This μ -value is more than three times higher than any other documented Martian reservoir. These results indicate either the Martian mantle is significantly more heterogeneous than previously thought (μ -value of 1–14 vs. 1–5) and/or the monzonitic

clasts formed by the melting of Martian crust with a μ -value of at least 13.4. Therefore, NWA 7533 may contain the first isotopic evidence for an enriched, differentiated crust on Mars.

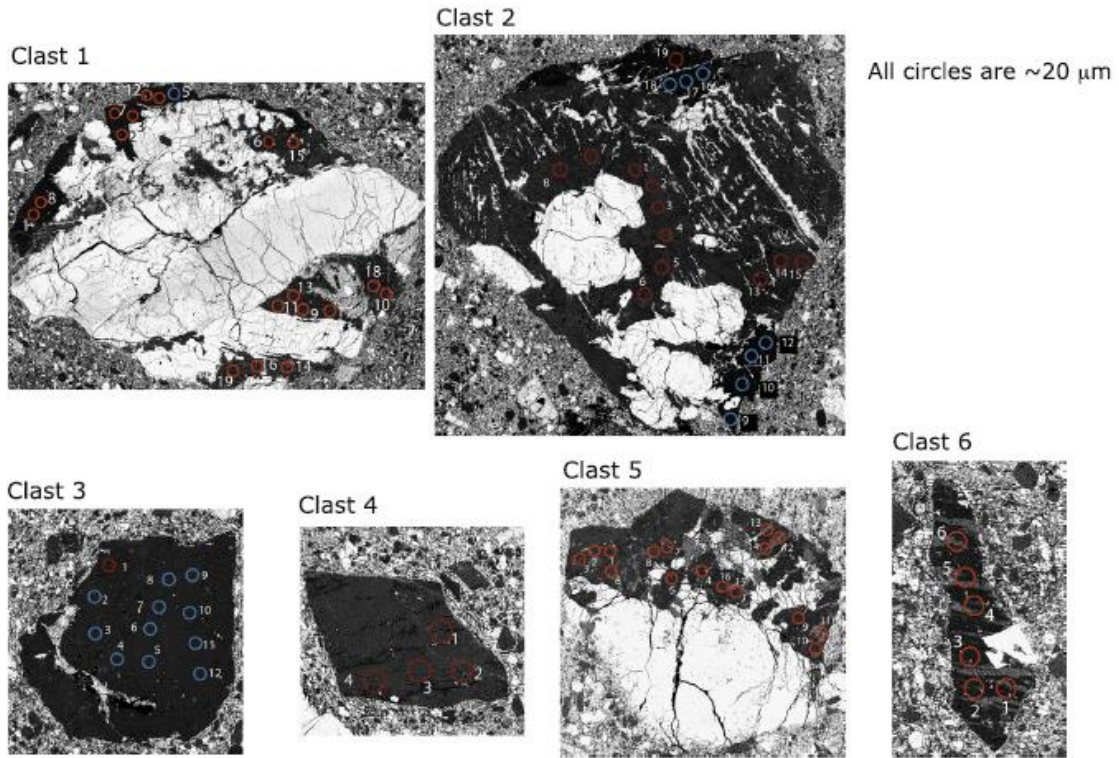


Figure 25: Clasts measured in study of Bellucci et al. (2015)

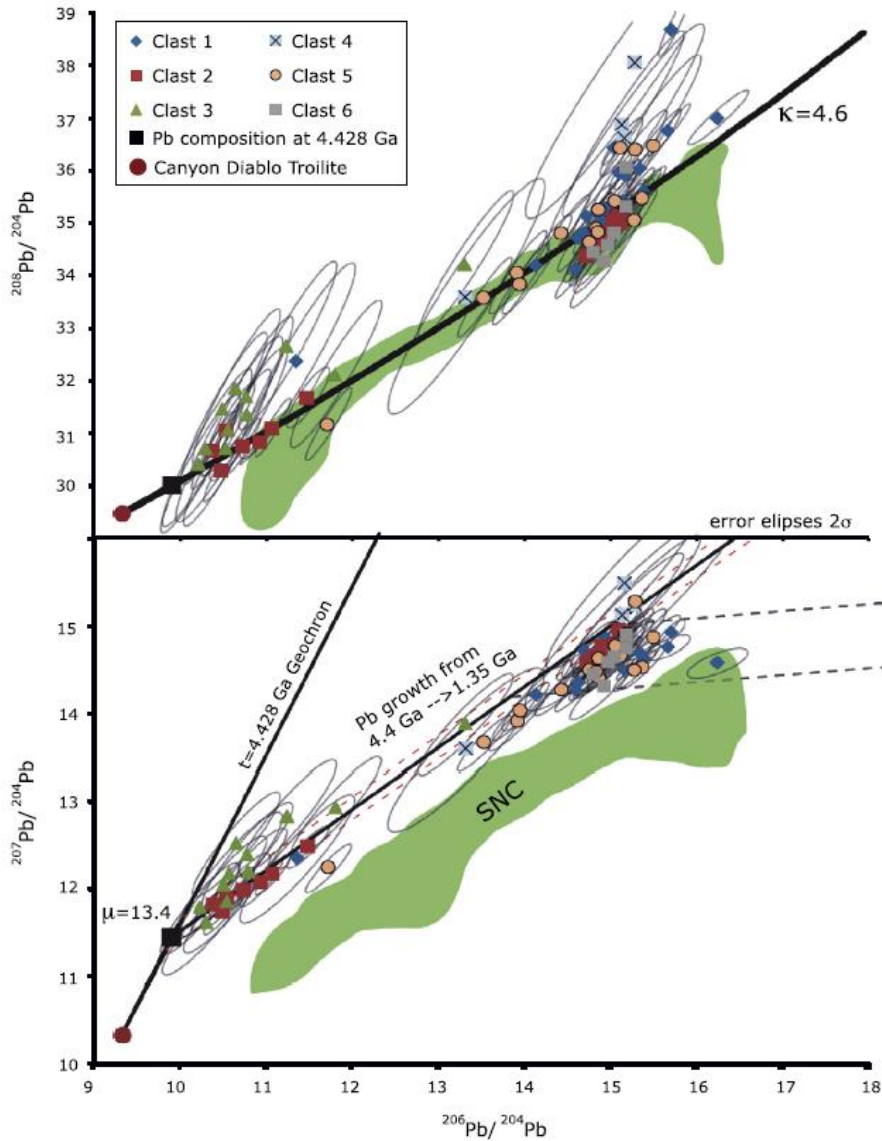


Figure 26: Pb isotopic results from study of Bellucci et al. (2015)

Formation ages for the sample reported by Cartwright et al. (2014) suggest events at ~ 1.6 Ga (K–Ar), and ~ 170 Ma (U–Th/He), which are considerably younger than those observed by Rb–Sr (2.1 Ga), and Sm–Nd (4.4 Ga; zircons ~ 4.4 Ga). However, their K–Ar age is similar to a disturbance in the U–Pb zircon data at ~ 1.7 Ga, which could hint that both chronometers have been subjected to disturbance by a common process or event. The U–Th/He age of ~ 170 Ma could relate to complete loss of radiogenic ^4He at this time, and is a similar age to the crystallization age of most shergottites. Although this could be coincidental, it might also indicate that shergottite formation and NWA7034 thermal metamorphism record a single thermal event.

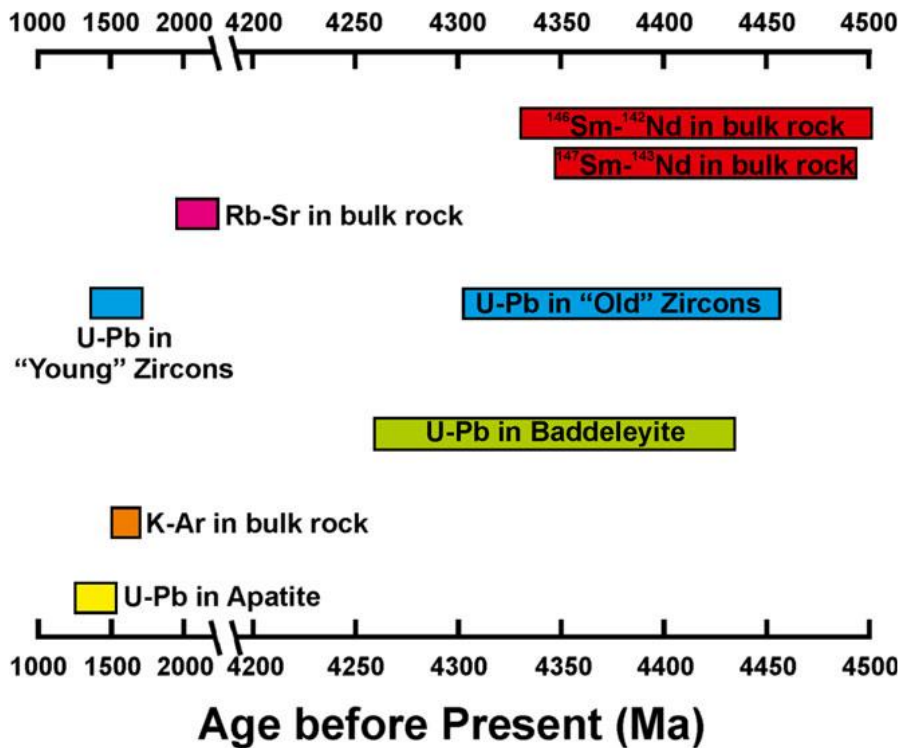


Figure 27: Age summary of NWA 7034 (from Nyquist et al., 2016).

Overall, the major age groupings for NWA 7034 and pairs, are as follows: 4.26 to 4.5 Ga recorded in U-Pb dating of zircons, baddeleyites and Sm-Nd in bulk rocks, followed by 1.3 to 1.7 Ga ages recorded by U-Pb in apatite, K-Ar in bulk rock, and U-Pb in younger zircons (Figure 27). The rocks may have formed in the 1.3 to 1.7 Ga age range, which would permit its origin from the northern hemisphere of Mars.

Noble gases and cosmogenic isotopes

Cartwright et al. (2014) report the first noble gas results for NWA7034, and show the presence of a trapped component resembling the current Martian atmosphere (Figure 28). This trapped component is also similar in composition to trapped gases found in the much younger shergottites (~150–600 Ma).

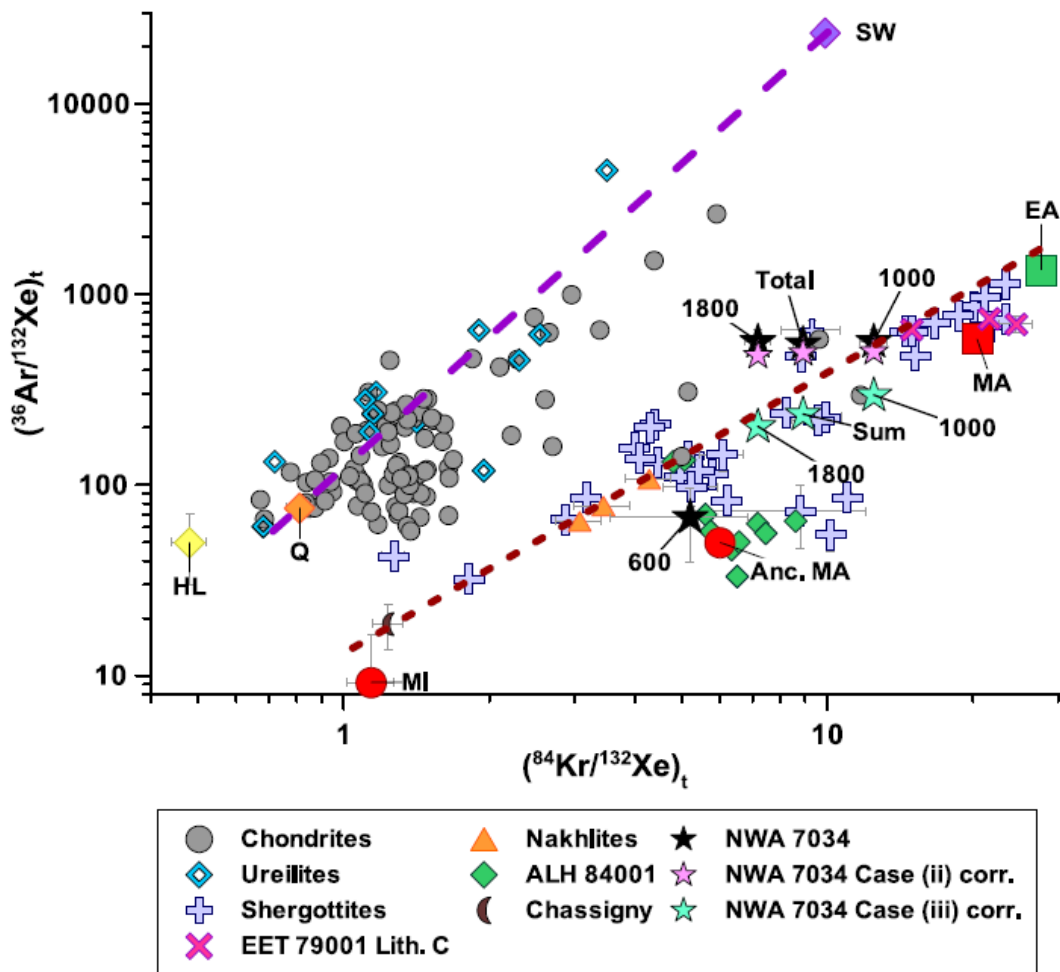


Figure 28: noble gas systematics of NWA 7034 compared to many other martian meteorites (from Cartwright et al., 2014).

As NWA7034 is a regolith breccia with multiple lithologies and a strong compositional similarity to Gusev soils, the timing and incorporation of trapped atmospheric gases is unclear. With hints of resetting events at ~1.5–2.1 Ga, the atmospheric component may have been incorporated during breccia formation – possibly in the Amazonian, though it could also have been incorporated on ejection from the surface.

Consideration of cosmic ray exposure ages, Cartwright et al. (2014) favor an age of ~5 Ma, which is outside the ranges for other Martian meteorite groups, and may suggest a distinct ejection event. Cosmogenic production rates and noble gas data are consistent with a meteoroid radius of >50 cm.

Other studies:

Magnetism

Among the 25 unpaired Martian meteorites studied to date, NWA 7034 has a unique magnetic mineralogy, and high saturation remanence magnetism (Figure 29). It contains about 15 wt % of iron oxides as magnetite that has experienced cation substitution and partial alteration to maghemite, with about a quarter of the oxides being pure maghemite. It also contains oxyhydroxides in the form of superparamagnetic goethite. The presence of maghemite and goethite, two purely ferric phases, makes NWA 7034 the most oxidized Martian meteorite, consistent with the presence of pyrite (Agee et al., 2013b). We associate this mineral assemblage with near-surface low-temperature hydrothermal alteration. The same hydrothermal alteration, possibly triggered by impact, may also be responsible for the formation of part of the magnetite.

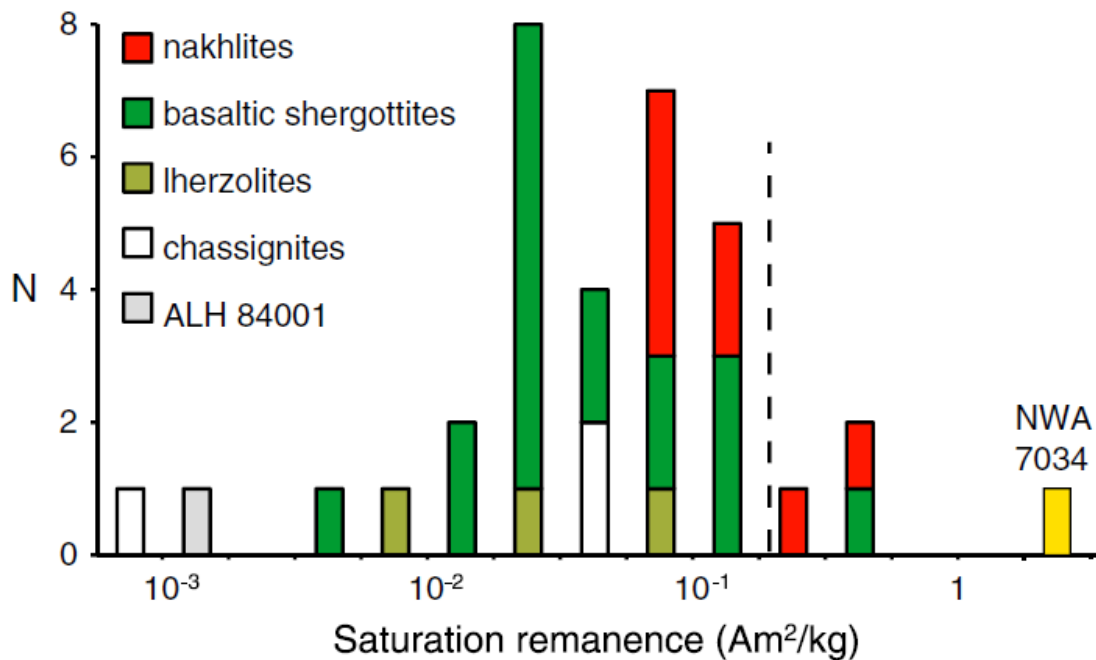


Figure 29: Saturation remanence for NWA 7034, showing its high value compared to many other martian meteorites (from Gattacceca et al., 2015).

Spectroscopy

NWA 7034 is spectrally distinct from all other SNC meteorites measured to date. It has a very low reflectance, low spectral contrast and a negative spectral slope across the VNIR (Figure 30), resembling OMEGA measurements of the dark plains (Poulet et al., 2009; Horgan and Bell, 2012). In the MIR NWA 7034 has a boxy reststrahlen region resembling TES measurements of ST1 low-albedo surfaces. All these characteristics are

more consistent with the average martian low-albedo regions than the SNCs, as determined by remotely sensed data. Low-albedo (dust-poor) regions on Mars are likely composed of a mixture of basaltic breccia, basalt, and basaltic glass that are all physically weathered on the surface to varying grain sizes. If this interpretation is correct then impacts have played a core role in shaping the martian regolith, as expected for heavily-cratered bodies lacking in plate tectonics and Venus-style global resurfacing.

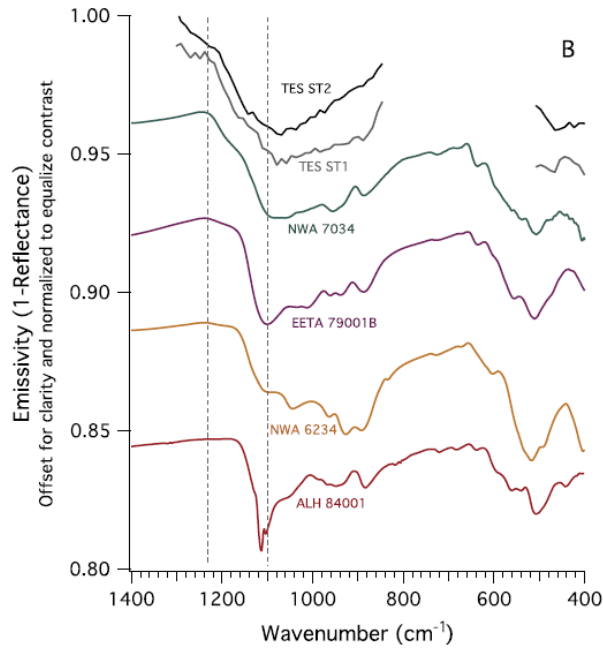


Figure 30: VNIR spectrum of NWA 7034 and other martian meteorites from the study of Cannon *et al.* (2015).

References for NWA7034

(originally compiled by C. Meyer, Oct 2012 and updated by K. Righter October 2017)

- Agee C.B. (2012) Heterogeneous Mars: Evidence from new unique Martian meteorite NWA 7034 *or maybe not Mars at all* (abs#6041) The Mantle of Mars WKS @ The LPI, Clear Lake
- Agee C.B., Wilson N.V., McCubbin F.M., Sharp Z.D. and Ziegler K. (2012a) Basaltic breccia NWA 7034: New ungrouped planetary achondrite (abs#2690) *43rd Lunar Planet. Sci. Conf.* Lunar Planetary Institute @ The Woodlands.
- Agee C.B., Wilson N.V., Polyak V.J., Ziegler K., McCubbin F.M., Asmeron Y., Sharp Z.D., Nunn M.H, Thiemens M.H. and Steele A. (2012b) Basaltic breccia NWA 7034: Unique 2.1 GA sample of enriched Martian crust (abs#5391). *75th Meteoritical Soc. @ Cairns*
- Agee, C. B., Wilson, N. V., McCubbin, F. M., Ziegler, K., Polyak, V. J., Sharp, Z. D., ... & Steele, A. (2013). Unique meteorite from early Amazonian Mars: Water-rich basaltic breccia Northwest Africa 7034. *Science*, 339(6121), 780-785.
- Agee, Carl. "BLACK BEAUTY: A UNIQUE 4.4 GA, WATER-RICH METEORITE FROM MARS." (2014): 168-168.
- Agee, C. B., McCubbin, F. M., Shearer, C. S., Santos, A. R., Burkemper, L. K., Provencio, P., & Wilson, N. V. (2013, March). Oxide phases and oxygen fugacity of Martian basaltic breccia Northwest Africa 7034. In *Lunar and Planetary Science Conference* (Vol. 44, p. 2965).
- Bellucci, J. J., Nemchin, A. A., Whitehouse, M. J., Humayun, M., Hewins, R., & Zanda, B. (2015). Pb-isotopic evidence for an early, enriched crust on Mars. *Earth and Planetary Science Letters*, 410, 34-41.
- Bellucci, J. J., Whitehouse, M. J., John, T., Nemchin, A. A., Snape, J. F., Bland, P. A., & Benedix, G. K. (2017). Halogen and Cl isotopic systematics in Martian phosphates: Implications for the Cl cycle and surface halogen reservoirs on Mars. *Earth and Planetary Science Letters*, 458, 192-202.
- Cannon, K. M., Mustard, J. F., & Agee, C. B. (2015). Evidence for a widespread basaltic breccia component in the martian low-albedo regions from the reflectance spectrum of Northwest Africa 7034. *Icarus*, 252, 150-153.
- Cartwright, J. A., Ott, U., Hermann, S., & Agee, C. B. (2013, March). NWA 7034 contains Martian atmospheric noble gases. In *Lunar and Planetary Science Conference* (Vol. 44, p. 2314).
- Cartwright, J. A., Ott, U., Herrmann, S., & Agee, C. B. (2014). Modern atmospheric signatures in 4.4 Ga Martian meteorite NWA 7034. *Earth and Planetary Science Letters*, 400, 77-87.
- Cassata, W. S. (2017). Meteorite constraints on Martian atmospheric loss and paleoclimate. *Earth and Planetary Science Letters*, 479, 322-329.

- Crowther, S. A., Jastrzebski, N. D., Nottingham, M., Theis, K. J., & Gilmour, J. D. (2014). NWA 8114: Analysis of Xenon in this Unique Martian Meteorite. *LPI Contributions, 1800*, 5316.
- Farquhar, J., Thiemens, M. H. & Jackson, T. (1998) Atmosphere surface interactions on Mars: $\delta^{17}\text{O}$ measurements of carbonate from ALH 84001. *Science* 280, 1580-1582.
- Franchi, I. A., Wright, I. P. & Pillinger, C. T. (1999) The oxygen isotope composition of Earth and Mars. *Meteorit. Planet. Sci.* 34, 657-661.
- Gattacceca, J., Rochette, P., Scorzelli, R. B., Munayco, P., Agee, C., Quesnel, Y., ... & Geissman, J. (2014). Martian meteorites and Martian magnetic anomalies: A new perspective from NWA 7034. *Geophysical Research Letters*, 41(14), 4859-4864.
- Goderis, S., Brandon, A. D., Mayer, B., & Humayun, M. (2016). Ancient impactor components preserved and reworked in martian regolith breccia Northwest Africa 7034. *Geochimica et Cosmochimica Acta*, 191, 203-215.
- Griffiths, A. A., Burgess, R., Joy, K. H., Lowe, T., & Withers, P. J. (2014). Petrography and Composition of Martian Meteorite Northwest Africa 8114. *LPI Contributions, 1800*, 5304.
- Hand, E. (2014). Martian obsession. *Science*, 346(6213), 1044-1049.
- Hewins, R. H., Zanda, B., Humayun, M., Nemchin, A., Lorand, J. P., Pont, S., ... & Marinova, M. (2017). Regolith breccia Northwest Africa 7533: Mineralogy and petrology with implications for early Mars. *Meteoritics & Planetary Science* 52, 89-124.
- Humayun, M. (2013). A unique piece of Mars. *Science*, 339(6121), 771-772.
- Humayun, M., Nemchin, A., Zanda, B., Hewins, R. H., Grange, M., Kennedy, A., ... & Deldicque, D. (2013). Origin and age of the earliest Martian crust from meteorite NWA [thin] 7533. *Nature*, 503(7477), 513-516.
- Kruijer, Thomas S., Thorsten Kleine, Lars E. Borg, Gregory A. Brennecka, Anthony J. Irving, Addi Bischoff, and Carl B. Agee. "The early differentiation of Mars inferred from Hf–W chronometry." *Earth and Planetary Science Letters* 474, 345-354.
- Leroux, H., Jacob, D., Marinova, M., Hewins, R. H., Zanda, B., Pont, S., ... & Humayun, M. (2016). Exsolution and shock microstructures of igneous pyroxene clasts in the Northwest Africa 7533 Martian meteorite. *Meteoritics & Planetary Science*, 51(5), 932-945.
- Liu, Y., Ma, C., Beckett, J. R., Chen, Y., & Guan, Y. (2016). Rare-earth-element minerals in martian breccia meteorites NWA 7034 and 7533: Implications for fluid–rock interaction in the martian crust. *Earth and Planetary Science Letters*, 451, 251-262.
- Lorand, J. P., Hewins, R. H., Remusat, L., Zanda, B., Pont, S., Leroux, H., ... & Grange, M. (2015). Nickeliferous pyrite tracks pervasive hydrothermal alteration in Martian regolith breccia: A study in NWA 7533. *Meteoritics & Planetary Science*, 50(12), 2099-2120.

- MacArthur, J. L., Bridges, J. C., Hicks, L. J., & Gurman, S. J. (2015, March). The Thermal and Alteration History of NWA 8114 Martian Regolith. In *Lunar and Planetary Science Conference* (Vol. 46, p. 2295).
- Magna, T., Yan H., Teng, F.-Z., and Mezger, K. (2017) Magnesium isotope systematics in Martian meteorites. *Earth and Planetary Science Letters* 474, 419-426.
- McCubbin, F. M., et al. (2016), Geologic history of Martian regolith breccia Northwest Africa 7034: Evidence for hydrothermal activity and lithologic diversity in the Martian crust, *J. Geophys. Res. Planets*, 121, 2120–2149, doi:10.1002/2016JE005143.
- Muttik, N., McCubbin, F. M., Keller, L. P., Santos, A. R., McCutcheon, W. A., Provencio, P. P., ... & Agee, C. B. (2014). Inventory of H₂O in the ancient Martian regolith from Northwest Africa 7034: The important role of Fe oxides. *Geophysical Research Letters*, 41(23), 8235-8244.
- Muttik, N., Keller, L. P., Agee, C. B., McCubbin, F. M., Santos, A. R., & Rahman, Z. (2014, March). A TEM Investigation of the Fine-Grained Matrix of Martian Basaltic Breccia NWA 7034. In *Lunar and Planetary Science Conference* (Vol. 45, p. 2763).
- Nemchin, A. A., Humayun, M., Whitehouse, M. J., Hewins, R. H., Lorand, J. P., Kennedy, A., ... & Deldicque, D. (2014). Record of the ancient martian hydrosphere and atmosphere preserved in zircon from a martian meteorite. *Nature Geoscience*, 7(9), 638-642.
- Nyquist, L. E., Shih, C. Y., Peng, Z. X., & Agee, C. (2013). NWA 7034 Martian breccia: Disturbed Rb-Sr systematics, preliminary ~ 4.4 Ga Sm-Nd age. *Meteoritics and Planetary Science Supplement*, 76, 5318.
- Nyquist, L. E., Shih, C. Y., McCubbin, F. M., Santos, A. R., Shearer, C. K., Peng, Z. X., ... & Agee, C. B. (2016). Rb-Sr and Sm-Nd isotopic and REE studies of igneous components in the bulk matrix domain of Martian breccia Northwest Africa 7034. *Meteoritics & Planetary Science* 51, 483–498.
- Rumble, D. & Irving, A. J. (2009) Dispersion of oxygen isotopic composition among 42 martian meteorites determined by laser fluorination: Evidence for assimilation of (ancient) altered crust. *Lunar Planet Sci.* **XL**, abstr. #2293.
- Santos, A. R., Agee, C. B., McCubbin, F. M., Shearer, C. K., Burger, P. V., Tartèse, R., & Anand, M. (2015). Petrology of igneous clasts in Northwest Africa 7034: Implications for the petrologic diversity of the martian crust. *Geochimica et Cosmochimica Acta*, 157, 56-85.
- Sharp, Z., Williams, J., Shearer, C., Agee, C., & McKeegan, K. (2016). The chlorine isotope composition of Martian meteorites 2. Implications for the early solar system and the formation of Mars. *Meteoritics & Planetary Science*. *Meteoritics & Planetary Science* 51, Nr 11, 2111–2126
- Steele, A., McCubbin, F. M., & Fries, M. D. (2016). The provenance, formation, and implications of reduced carbon phases in Martian meteorites. *Meteoritics & Planetary Science*, 51(11), 2203-2225.

- Stephenson, P. C., Lin, Y., & Leya, I. (2017). The noble gas concentrations of the Martian meteorites GRV 99027 and paired NWA 7906/NWA 7907. *Meteoritics & Planetary Science*. DOI: 10.1111/maps.12950.
- Tarte`se, R., Anand, M., McCubbin, F. M., Santos, A. R. and Delhaye, T. (2014) Zircons in Northwest Africa 7034: recorders of crustal evolution on Mars. 45th Lunar Planet. Sci. Conf. #2020.
- Udry, A., Lunning, N. G., McSween, H. Y., & Bodnar, R. J. (2014). Petrogenesis of a vitrophyre in the martian meteorite breccia NWA 7034. *Geochimica et Cosmochimica Acta*, 141, 281-293.
- Williams, J. T., C. K. Shearer, Z. D. Sharp, P. V. Burger, F. M. McCubbin, A. R. Santos, C. B. Agee, and K. D. McKeegan. "The chlorine isotopic composition of Martian meteorites 1: Chlorine isotope composition of Martian mantle and crustal reservoirs and their interactions." *Meteoritics & Planetary Science* 51, no. 11 (2016): 2092-2110.
- Wieler, R., Huber, L., Busemann, H., Seiler, S., Leya, I., Maden, C., ... & Irving, A. J. (2016). Noble gases in 18 Martian meteorites and angrite Northwest Africa 7812—Exposure ages, trapped gases, and a re-evaluation of the evidence for solar cosmic ray-produced neon in shergottites and other achondrites. *Meteoritics & Planetary Science* 51, 407-428.
- Wittmann, A., Korotev, R. L., Jolliff, B. L., Irving, A. J., Moser, D. E., Barker, I., & Rumble, D. (2015). Petrography and composition of Martian regolith breccia meteorite Northwest Africa 7475. *Meteoritics & Planetary Science* 50, 326-352.
- Yin, Q.-Z., McCubbin, F. M., Zhou, Q., Santos, A. R., Tarte`se, R., Li, X., Li, Q., Liu, Y., Tang, G., Boyce, J. W., Lin, Y., Yang, W., Zhang, J., Hao, J., Elardo, S. M., Shearer, C. K., Rowland, D. J., Lerche, M. and Agee, C. B. (2014) An Earth-like beginning for ancient Mars indicated by alkali-rich volcanism at 4.4 Ga. 45th Lunar Planet. Sci. Conf. #1320.
- Ziegler, K., Sharp, Z.D., and Agee, C.B. (2013) The unique NWA 7034 martian meteorite: Evidence for multiple oxygen isotope reservoirs. *Lunar Planet Sci.* **XLXV**, abstr. #2639.